Proceedings of the 8th International Conference on Multiphase Flow and Heat Transfer (ICMFHT'23)
Lisbon, Portugal – March 26 – 28, 2023
Paper No. ICMFHT 112
DOI: 10.11159/icmfht23.112

Numerical Simulation of the Effect of Temperature on Binary Alkane Mixture Segregation using a Mass Transfer Cavitation Model

Philip Schwarz[1], Romuald Skoda[1]
[1]Chair of Hydraulic Fluid Machinery, Ruhr University Bochum
Universitätsstr. 150, 44801 Bochum, Germany
philip.schwarz@ruhr-uni-bochum.de; romuald.skoda@ruhr-uni-bochum.de

Abstract **-** A mass transfer cavitation model for binary alkane mixtures is proposed, implemented into the in-house CFD code hydRUB and applied to a hydrofoil test case. A binary *n*-dodecane/*n*-heptane mixture at two different temperatures is considered. The saturation pressure of *n*-heptane and *n*-dodecane differs more than two orders of magnitude, so the evaporation rate of the lighter *n*-heptane is much higher than the one of the heavier *n*-dodecane. Therefore, cavitation leads to an enrichment of *n*-heptane in the vapor phase. This is associated with a slight densification, i.e., enrichment of *n*-dodecane in the liquid phase, which means that local segregation of both species occurs. With increasing temperature, the amount of *n*-dodecane in the vapor phase is substantially increased since the saturation pressures of both species approach. Therefore, species mass transfer deviates much less and segregation is less pronounced for the higher temperature compared to the lower one.

Keywords**:** Binary Alkane Mixture, Cavitation, Species segregation, Temperature Influence, Multiphase, Mass Transfer, 3D CFD

1. Introduction

In hydraulic systems, cavitation can lead to complications such as noise, vibration, and cavitation erosion. A distinctive feature of these systems is the working fluid, e.g., fuel, which consists of several hundred species. In addition to temperature and pressure, thermophysical properties of a mixture also depend on local composition. In 3D Computational Fluid Dynamics (CFD) approaches for cavitating flow, single-species surrogate fluids are usually utilized as working fluids. For example, [1 - 7] utilized a pure alkane or a single-species surrogate fluid to approximate the properties of fuel.

For single-species surrogate fluids it is assumed that the composition of the mixture is invariant so that the properties of the fluid solely depend on temperature and pressure. Local property changes due to a locally varying fluid composition are neglected. However, in experimental studies by [8] and [9] on cavitating fuel significant differences in cavitation structures occurred compared to single-species, which may indicate that local segregation of the fuel was occurring. As pointed out by [9], the saturation pressure of individual species in fuel varies by three orders of magnitude. This in turn may be associated with a staggered evaporation and re-condensation of the individual species, i.e., a local segregation of species. Since the saturation pressure is also temperature dependent, we suppose that temperature may significantly impact the segregation process.

Few simulation studies consider a cavitating mixture of multi-species and their segregation. [10] and [11] studied the injection of mixtures under supercritical and transcritical conditions. [12] focused on a high-pressure injection of an alkane mixture into nitrogen but did not present local concentration of the species. [13 - 15] investigated vapor-liquid equilibrium of multi-species mixtures, but no spatially resolved fuel concentration was given. Furthermore, [16] presented saturation curves of multi-species mixtures and their changes due to fuel segregation. In contrast to a pure species, the saturation temperature increased due to successive evaporation of the high-volatile species and densification of the remaining liquid. All cited studies applied homogeneous equilibrium models, which assume a very rapid relaxation process of pressure, temperature, and chemical potential. The time required to reach thermodynamic equilibrium is assumed to be much smaller than the numerically resolved hydrodynamic time scales [17]. However, studies by [18 - 20] indicate that relaxation times might be significant.

In this study, we propose a mass transfer cavitation model for binary mixtures. Therefore, we consider an *n*-heptane/*n*-dodecane mixture flow over a NACA 0015 hydrofoil and a temperature variation. Phase transition from liquid to vapor phase

and vice versa is considered by a source term in the vapor mass fraction transport equation, as an extension of the cavitation model of [21]. We assume kinetic, mechanical, and thermal equilibrium and a homogeneous distribution of all species in the computational cell, while a vapor mass source term replaces the chemical equilibrium assumption.

2. Model formulation

We propose the solution of conservation of mixture mass, mixture momentum, and mixture energy. Furthermore, we introduce a transport equation for mass fraction of species (index 1) $Y_1 = m_1/m$ and vapor (index v) $Y_v = m_v/m$, where mass m refers to a CFD cell. The equations are given by

$$\frac{\partial \rho}{\partial t} + \mathrm{div}(\rho\, \mathbf{u}) = 0\,, \tag{1}$$

$$\frac{\partial \rho}{\partial t} + \mathrm{div}(\rho \boldsymbol{u} \otimes \boldsymbol{u} + p\mathbf{I}) = \mathbf{0}\,, \tag{2}$$

$$\frac{\partial E_{\mathrm{tot}}}{\partial t} + \mathrm{div}(H_{\mathrm{tot}}\boldsymbol{u}) = 0\,, \tag{3}$$

$$\frac{\partial \rho Y_1}{\partial t} + \mathrm{div}(\rho Y_1 \boldsymbol{u}) = 0\,, \qquad \text{and} \tag{4}$$

$$\frac{\partial \rho Y_v}{\partial t} + \mathrm{div}(\rho Y_v \boldsymbol{u}) = \dot{m}\,, \tag{5}$$

where t is time, ρ is density, $\boldsymbol{u}$ is velocity, p is pressure, and E_{tot} and H_{tot} are total energy and enthalpy of the mixture. Viscous effects and interdiffusion of species within each phase are neglected. Furthermore, $\dot{m}$ is the mass relaxation term described by the bubble dynamic mass transfer cavitation model introduced in the following.

The model for mass transfer is adopted from [21], where the vapor phase is assumed to consist of homogeneously dispersed bubbles in the liquid, which are small compared to the computational cell. Mass transport is based on a simplified assumption for bubble growth in terms of the Rayleigh equation [22]. In our study, the far-field pressure in the fluid around the bubble and the local pressure inside the bubble are determined by the local CFD cell pressure p and the equilibrium pressure p_{eq}, respectively. We refer to the pressure at which two mixture phases are in equilibrium as p_{eq}. According to [23], the mass transfer term $\dot{m}$ as introduced by [21] is written as

$$\dot{m} = \alpha_\ell(1-\alpha_\ell)\sqrt{6\rho_\ell}\frac{\rho_v}{\rho}\frac{\sqrt{|p_{\mathrm{eq}} - p|}}{r}\,\mathrm{sign}\big(p_{\mathrm{eq}} - p\big)\,, \tag{6}$$

where α_ℓ is the volume fraction of the liquid phase, ρ_ℓ and ρ_v are the density of the liquid (index ℓ) and vapor phase, and r is the bubble radius.

A liquid-vapor mixture of two species in two phases comprises a system of three fluids. The mixing rules for density ρ and specific internal energy e are obtained using mixing theory (see, e.g., [24]) and are closed by the Noble-Abel Stiffened-Gas Equations of State (NASG-EOS) [25]. The NASG-EOS parameters for *n*-heptane and *n*-dodecane are evaluated by a minimization method by [25] to best match experimental data by [26]. The local composition of the phases is determined by Rault's and Dalton's law as

$$p_{v,j} = x_{\ell,j}\, p_{\mathrm{sat},j} \qquad \text{and} \tag{7}$$

$$p_{v,j} = x_{v,j}\, p_{\mathrm{eq}}\,, \tag{8}$$

where $p_{\mathrm{sat},j}$ is the saturation pressure and $p_{v,j}$ is the partial pressure in the vapor phase for species $j = n$-dodecane (dod) or n-heptane (hep). The partial mole fraction $x_{i,j} = n_{i,j}/n_i$ relates the amount of substance of species in the respective phase $n_{i,j}$ to the amount of substance of the respective phase n_i for $i = \ell$ or v. $p_{\mathrm{sat},j}$ is obtained by the NASG-EOS and by using basic thermodynamic relationships the system of equations is closed. The equilibrium pressure p_{eq} is used in Eq. (6) and constitutes the extension of the cavitation model source term from a single species to a species mixture.

Fig. 1 shows the phase diagram for an *n*-dodecane/*n*-heptane mixture, where Eq. (7) and Eq. (8) are evaluated for two different temperatures, i.e., 300 K and 350 K. The partial mass fraction $y_{i,j} = m_{i,j}/m_i$ is introduced accordingly to $x_{i,j}$. For example, a species mass fraction of $Y_{\mathrm{dod}} = Y_{\mathrm{hep}} = 0.5$ is marked. For a small amount of vapor, it consists of *n*-heptane to the very largest extent for both temperatures. The temperature difference of 50 K yields an increase of equilibrium pressure of about one order of magnitude (indicated by Δp_{eq} in Fig. 1) and an increase of *n*-dodecane content in vapor phase of the mixture $y_{v,\mathrm{dod}}$ by a factor of four (indicated by $\Delta y_{v,\mathrm{dod}}$ in Fig. 1).

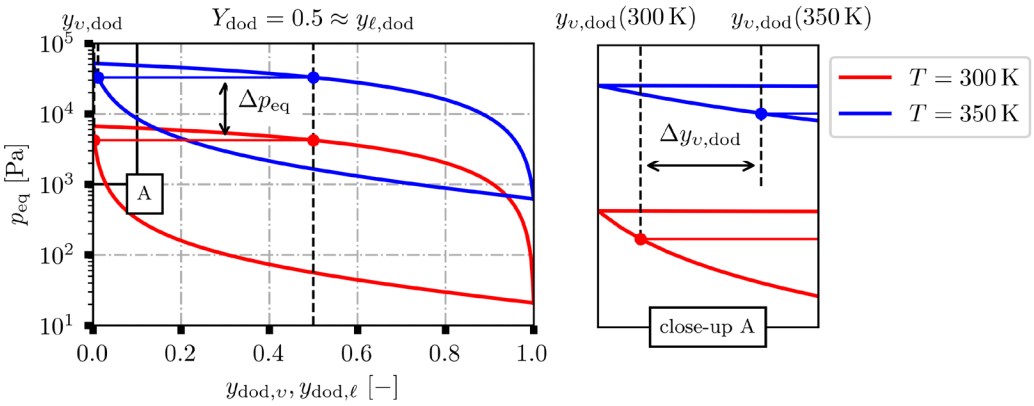

Fig. 1: Isothermal phase diagram of *n*-dodecane/*n*-heptane VLE at 300 K and 350 K.

3. Simulation method

The in-house CFD code hydRUB [3, 27 - 29] is utilized. Finite volume discretization with collocated variable storage in the cell center is applied in a compressible density-based solver. An inviscid low-Mach-number consistent numerical Godunov flux function in combination with an optimized four-stage low storage explicit Runge–Kutta time scheme [30, 31, 32] is applied. Second-order accuracy in space is achieved by reconstruction with the monotonic Total Variation Diminishing limiter MINMOD [33]. First, the mass relaxation term $\dot{m}$ in Eq. (6) and the composition of the single phases using Eq. (7) and Eq. (8) are determined. Thereafter, the conservation equations Eq. (1) to Eq. (5) are solved. Finally, the EOS is employed to calculate the primitive variables from the conservative ones.

4. Results

An unsteady 2D cavitating flow of a binary alkane mixture over a NACA 0015 hydrofoil is considered in the following. We adopt the case of [21] with an angle of attack of 6°, a cavitation number $\sigma = (p - p_{\mathrm{eq}})/(1/2\rho_\ell u^2) = 1$, and an Euler number of $\mathrm{Eu} = (p_{\mathrm{in}} - p_{\mathrm{out}})/(1/2\rho_\ell u_{\mathrm{in}}^2) \approx 2.4$. In contrast to [21] we use a *n*-dodecane/*n*-heptane mixture as working fluid. Two different temperatures, i.e., 300 K and 350 K, with a species mass fraction of $Y_{\mathrm{dod}} = Y_{\mathrm{hep}} = 0.5$ are studied. A CFL number of $\mathrm{CFL} \leq 0.9$ and a computational grid with 180×30 cells is employed.

In Fig. 2, the simulation results are presented in terms of vapor mass fraction Y_v, partial mass fraction of *n*-dodecane in liquid and vapor phase $y_{\ell,\mathrm{dod}}$ and $y_{v,\mathrm{dod}}$, as well as *n*-dodecane mass transfer rate related to the entire mass transfer rate $\dot{m}_{\mathrm{dod}}/\dot{m}$. An example time step within the periodic cavitation shedding cycles is shown. For 300 K, in the cavity at the leading edge vapor mass fraction rises to $Y_v \approx 0.02$ (Fig. 2a). A look at $y_{v,\mathrm{dod}}$ (Fig. 2b) reveals an essentially constant value of $y_{v,\mathrm{dod}} \approx 0.003$ within the cavity, which means that vapor consists of about 99.7 % *n*-heptane at any location irrespective of the amount of vapor. Vapor contains a larger amount of *n*-heptane due to its high volatility in terms of high saturation pressure $p_{\mathrm{sat,hep}}$, which means that *n*-dodecane evaporation rate is low (Fig. 2c). A constant $y_{v,\mathrm{dod}}$ distribution is substantiated by $\dot{m}_{\mathrm{dod}}/\dot{m} \approx 0.003$ (Fig. 2c), whose spatial variation is also insignificant. The significantly higher mass

transfer of *n*-heptane compared to *n*-dodecane leads to segregation in the liquid phase, which is illustrated by $y_{\ell,\mathrm{dod}}$ (Fig. 2d). The liquid is enriched by *n*-dodecane, indicated by regions with $y_{\ell,\mathrm{dod}} > 0.5$.

For 350 K, Y_v slightly increases (Fig. 2e). Albeit the difference of Y_v to the colder case is low, the vapor composition changes significantly. In the vapor phase $y_{v,\mathrm{dod}} \approx 0.01$ (Fig. 2f) and $\dot{m}_{\mathrm{dod}}/\dot{m} \approx 0.01$ (Fig. 2h), i.e., the content of *n*-dodecane increases about one order of magnitude. Enrichment of *n*-dodecane in the liquid phase and, therefore, segregation is slightly stronger for the higher temperature.

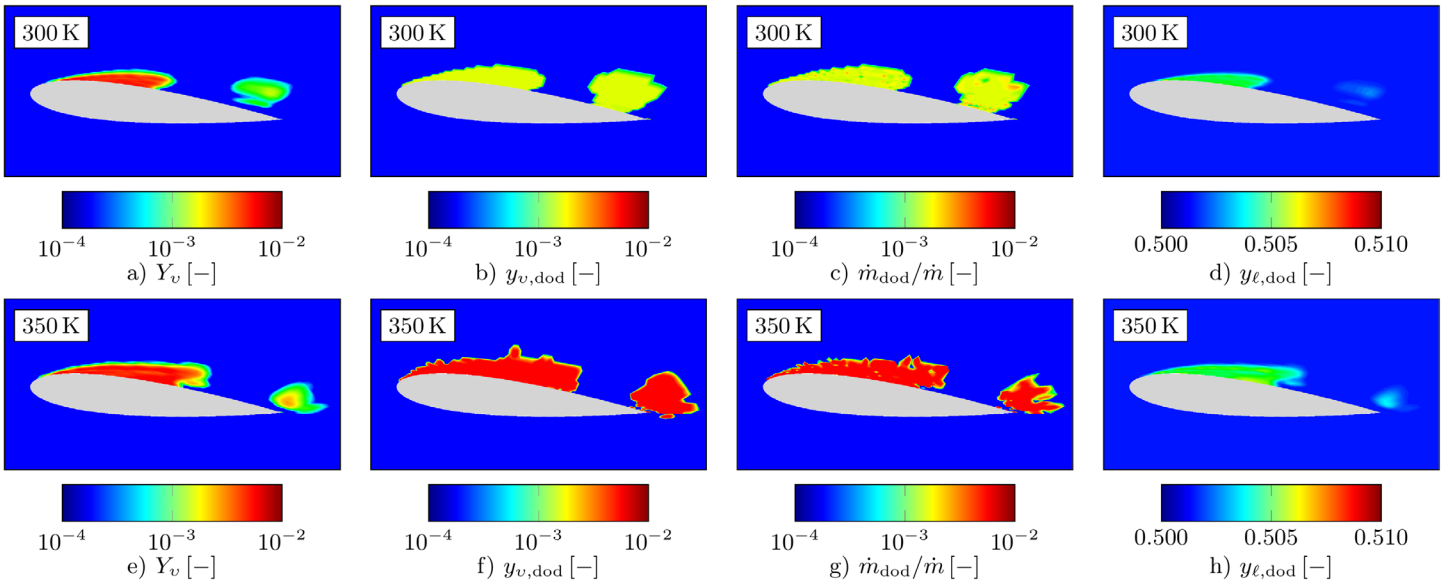

Fig. 2: Example shedding cycle time step for a n-octane/n-heptane mixture flow around a NACA 0015 hydrofoil for 300 K and 350 K. (a, e) Vapor mass fraction, (b, f) partial vapor mass fraction of *n*-dodecane, (c, g) ratio of *n*-dodecane mass transfer, and (d, h) partial liquid mass fraction of *n*-dodecane.

5. Conclusion

A cavitation model to account for species segregation in binary alkane mixture has been proposed and applied to a hydrofoil test case. The composition of the vapor phase is substantially affected by temperature. Local segregation, which is a deviation from the initial liquid mixture composition, is traced back to different mass transfer rates of both species during evaporation. Since the total amount of vapor is small in the considered case, the densification of liquid phase is low, which means that segregation affects a deviation from the initial liquid mass fraction by less than 1 %. We trace this moderate value back to the observation that considering a single bubble, segregation is confined to the proximity of the liquid-bubble interface, where it can rise to a considerably higher level, according to [34]. However, the phase interphase is not resolved by our homogeneous mixture approach and we observe a smearing effect of local segregation at the interfaces of the bubbles averaged over the computational cell.

References

[1] E. Giannadakis, D. Papoulias, A. Theodorakakos, and M. Gavaises, "Simulation of cavitation in outward-opening piezo-type pintle injector nozzles," *Proceedings of the Institution of Mechanical Engineers, Part D: Journal of Automobile Engineering*, vol. 222, no. 10, pp. 1895–1910, 2008.

[2] E. Giannadakis, M. Gavaises, and C. Arcoumanis, "Modelling of cavitation in diesel injector nozzles," *Journal of Fluid Mechanics*, vol. 616, pp. 153–193, 2008.

[3] R. Skoda, U. Iben, M. Güntner, and R. Schilling, "Comparison of compressible explicit density-based and implicit pressure-based cfd methods for the simulation of cavitating flows," in *Proceedings of the 8th International Symposium on Cavitation*, Singapore, August 2012.

[4] A. Theodorakakos, G. Strotos, N. Mitroglou, C. Atkin, and M. Gavaises, "Friction-induced heating in nozzle hole micro-channels under extreme fuel pressurisation," *Fuel*, vol. 123, pp. 143–150, 2014.

[5] P. Koukouvinis, M. Gavaises, J. Li, and L. Wang, "Large Eddy Simulation of Diesel injector including cavitation effects and correlation to erosion damage," *Fuel*, vol. 175, pp. 26–39, 2016.

[6] F. Örley, S. Hickel, S. J. Schmidt, and N. A. Adams, "Large-eddy simulation of turbulent, cavitating fuel flow inside a 9-hole diesel injector including needle movement," *International Journal of Engine Research*, vol. 18, no. 3, pp. 195–211, 2017.

[7] P. Schwarz, M. Blume, L. Weiß, M. Wensing, and R. Skoda, "3d simulation of a ballistic direct injection cycle for the assessment of fuel property effects on cavitating injector internal flow dynamics and primary breakup," *Fuel*, vol. 308, p. 121775, 2022.

[8] I. E. Dorofeeva, F. O. Thomas, and P. F. Dunn, "Cavitation of JP-8 Fuel in a Converging-Diverging Nozzle: Experiments and Modelling," in *Proceedings of the 7th International Symposium on Cavitation*, Ann Arbor (Michigan), USA, August 2009.

[9] P. F. Dunn, F. O. Thomas, M. P. Davis, and I. E. Dorofeeva, "Experimental characterization of aviation-fuel cavitation," *Physics of Fluids*, vol. 22, no. 11, p. 117102, 2010.

[10] C. Rodriguez, A. Vidal, P. Koukouvinis, M. Gavaises, and M. A. McHugh, "Simulation of transcritical fluid jets using the PC-SAFT EoS," *Journal of Computational Physics*, vol. 374, pp. 444–468, 2018.

[11] C. Rodriguez, P. Koukouvinis, and M. Gavaises, "Simulation of supercritical diesel jets using the pc-saft eos," *The Journal of Supercritical Fluids*, vol. 145, pp. 48–65, 2019.

[12] C. Rodriguez, H. B. Rokni, P. Koukouvinis, A. Gupta, and M. Gavaises, "Complex multicomponent real-fluid thermodynamic model for high-pressure diesel fuel injection," *Fuel*, vol. 257, p. 115888, 2019.

[13] A. Vidal, P. Koukouvinis, and M. Gavaises, "Effect of diesel injection pressures up to 450mpa on in-nozzle flow using realistic multicomponent surrogates," in *Proceedings of the 29th European Conference on Liquid Atomization and Spray Systems*, Paris, France, August 2019.

[14] A. Vidal, K. Kolovos, M. R. Gold, R. J. Pearson, P. Koukouvinis, and M. Gavaises, "Preferential cavitation and friction-induced heating of multi-component diesel fuel surrogates up to 450mpa," *International Journal of Heat and Mass Transfer*, vol. 166, p. 120744, 2021.

[15] K. Kolovos, P. Koukouvinis, R. M. McDavid, and M. Gavaises, "Transient cavitation and friction-induced heating effects of diesel fuel during the needle valve early opening stages for discharge pressures up to 450 mpa," *Energies*, vol. 14, no. 10, 2021.

[16] A. Vidal, C. Rodriguez, P. Koukouvinis, M. Gavaises, and M. A. McHugh, "Modelling of diesel fuel properties through its surrogates using perturbed-chain, statistical associating fluid theory," *International Journal of Engine Research*, vol. 21, no. 7, pp. 1118–1133, 2020.

[17] J. Matheis and S. Hickel, "Multi-component vapor-liquid equilibrium model for les of high-pressure fuel injection and application to ecn spray a," *International Journal of Multiphase Flow*, vol. 99, pp. 294–311, 2018.

[18] Z. Bilicki, J. Kestin, and J. T. Stuart, "Physical aspects of the relaxation model in two-phase flow," *Proceedings of the Royal Society of London. A. Mathematical and Physical Sciences*, vol. 428, no. 1875, pp. 379–397, 1990.

[19] P. Downar-Zapolski, Z. Bilicki, L. Bolle, and J. Franco, "The non-equilibrium relaxation model for one-dimensional flashing liquid flow," *International Journal of Multiphase Flow*, vol. 22, no. 3, pp. 473–483, 1996.
[20] D. Schmidt, S. Gopalakrishnan, and H. Jasak, "Multi-dimensional simulation of thermal non-equilibrium channel flow," *International Journal of Multiphase Flow*, vol. 36, no. 4, pp. 284–292, 2010.
[21] G. H. Schnerr and J. Sauer, "Physical and numerical modeling of unsteady cavitation dynamics," in *Proceedings of the 4th International Conference on Multiphase Flow*, New Orleans (Louisiana), USA, June 2001.
[22] M. S. Plesset and A. Prosperetti, "Bubble Dynamics and Cavitation," *Annual Review of Fluid Mechanics*, vol. 9, pp. 145–185, 1977.
[23] C. Deimel, M. Günther, and R. Skoda, "Application of a pressure based CFD code with mass transfer model based on the Rayleigh equation for the numerical simulation of the cavitating flow around a hydrofoil with circular leading edge," in *European Physical Journal Web of Conferences*, vol. 67, 2014, p. 02018.
[24] S. Dellacherie, "Relaxation schemes for the multicomponent euler system," *ESAIM: Mathematical Modelling and Numerical Analysis*, vol. 37, no. 6, pp. 909–936, 2003.
[25] O. Le Métayer and R. Saurel, "The noble-abel stiffened-gas equation of state," *Physics of Fluids*, vol. 28, no. 4, p. 046102, 2016.
[26] E. W. Lemmon, M. O. McLinden, and D. G. Friend, "Thermophysical properties of fluid systems," in *NIST Chemistry WebBook, NIST Standard Reference Database 69*, P. Linstrom and W. Mallard, Eds. National Institute of Standards and Technology, Gaithersburg MD, 20899, 2021.
[27] R. Skoda, U. Iben, A. Morozov, M. Mihatsch, S. Schmidt, and N. Adams, "Numerical simulation of collapse induced shock dynamics for the prediction of the geometry, pressure and temperature impact on the cavitation erosion in micro channels," in *Proceedings of the 3rd International Cavitation Forum*, Coventry, United Kingdom, July 2011.
[28] S. Mottyll and R. Skoda, "Numerical 3d flow simulation of ultrasonic horns with attached cavitation structures and assessment of flow aggressiveness and cavitation erosion sensitive wall zones," *Ultrasonics Sonochemistry*, vol. 31, pp. 570–589, 2016.
[29] M. Hosbach, R. Skoda, T. Sander, U. Leuteritz, and M. Pfitzner, "On the temperature influence on cavitation erosion in micro-channels," *Experimental Thermal and Fluid Science*, vol. 117, p. 110140, 2020.
[30] S. Schmidt, I. Sezal, G. Schnerr, and M. Thalhamer, "Compressible simulation of liquid/vapor two-phase flows with local phase transition," in *Proceedings of the 6th International Conference on Multiphase Flow*, Leipzig, Germany, July 2007.
[31] S. Schmidt, I. Sezal, G. Schnerr, and M. Talhamer, "Riemann techniques for the simulation of compressible liquid flows with phase-transistion at all mach numbers - shock and wave dynamics in cavitating 3-d micro and macro systems," in *Proceedings of the 46th AIAA Aerospace Sciences Meeting and Exhibit*, Reno (Nevada), USA, January 2008.
[32] G. Schnerr, I. Sezal, and S. Schmidt, "Numerical investigation of three-dimensional cloud cavitation with special emphasis on collapse induced shock dynamics," *Physics of Fluids*, vol. 20, 2008.
[33] A. Harten, "High resolution schemes for hyperbolic conservation laws," *Journal of Computational Physics*, vol. 49, no. 3, pp. 357–393, 1983.
[34] J. Bermudez-Graterol and R. Skoda, "Numerical simulation of bubble dynamics and segregation in binary heptane/dodecane mixtures," *Journal of Fluid Mechanics*, vol. 947, p. A9, 2022.